SUPPLEMENTAL ONLINE MATERIAL

Kinetic isotope effects on hydrogen/deuterium atom disordering and ordering in ice crystals: A Raman and dielectric study of ice VI, XV, and XIX

Alexander V. Thoeny[1], Tobias M. Gasser[1], Lars Hoffmann[2], Markus Keppler[2], Roland Böhmer[2], Thomas Loerting[1,*]

[1] *Institute of Physical Chemistry, University of Innsbruck, 6020 Innsbruck, Austria*
[2] *Fakultät Physik, Technische Universität Dortmund, 44221 Dortmund, Germany*
e-mail: thomas.loerting@uibk.ac.at

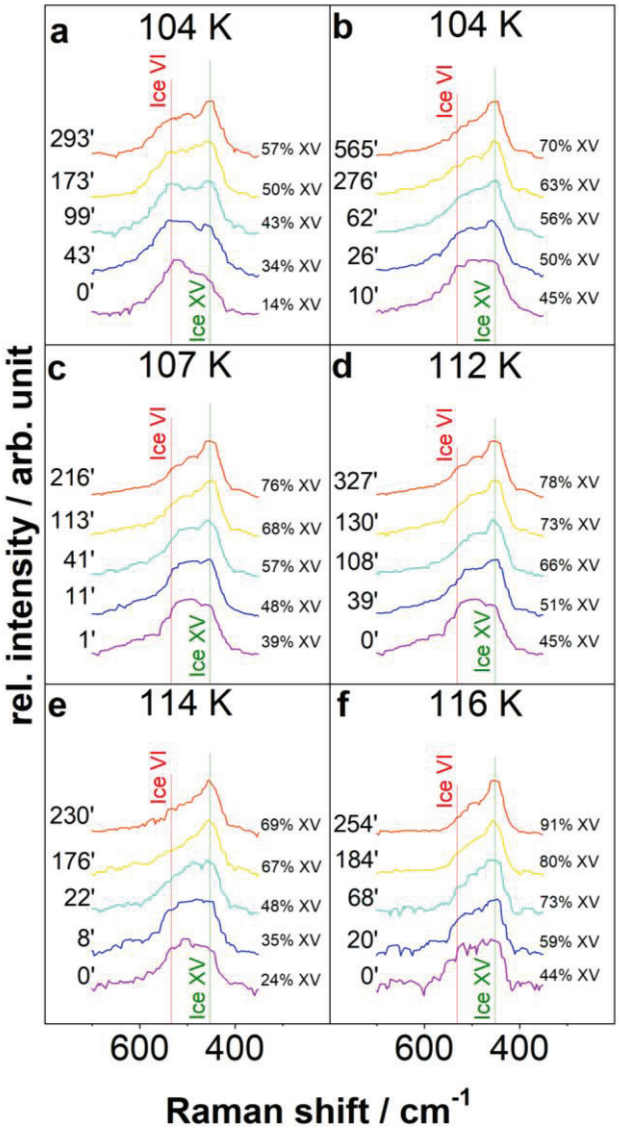

Figure S1: Ice XV buildup measured through the Raman librational bands of 95% H_2O samples at different temperatures. The spectra are marked with the time passed in the isothermal experiment and the result of the superposition analysis.

Dielectric spectroscopy is also useful to determine the rate constants of the ice VI‡ → XV transition. Dielectric isothermal waiting experiments were previously carried out, *e.g.*, for the transition from unrelaxed HDA to low-density amorphous ice [S1] or for the transition from stacking-disordered ice to hexagonal ice [S2]. For the present isothermal waiting experiments, the first data point for which the temperature stability was better than ±0.2 K is defined as t=0.

Dielectric loss spectra from the 95% H_2O sample, recorded for different times after stabilizing the temperature at 114 K, are shown in the inset of Fig. S2. As marked by the vertical line in the figure, a frequency of 133 Hz has been chosen to track the spectral changes with time. After normalizing the corresponding ε'' values, they are depicted in Fig. S2. The results from the fits using eq. (2) are represented by the solid lines and are compiled in Table S1.

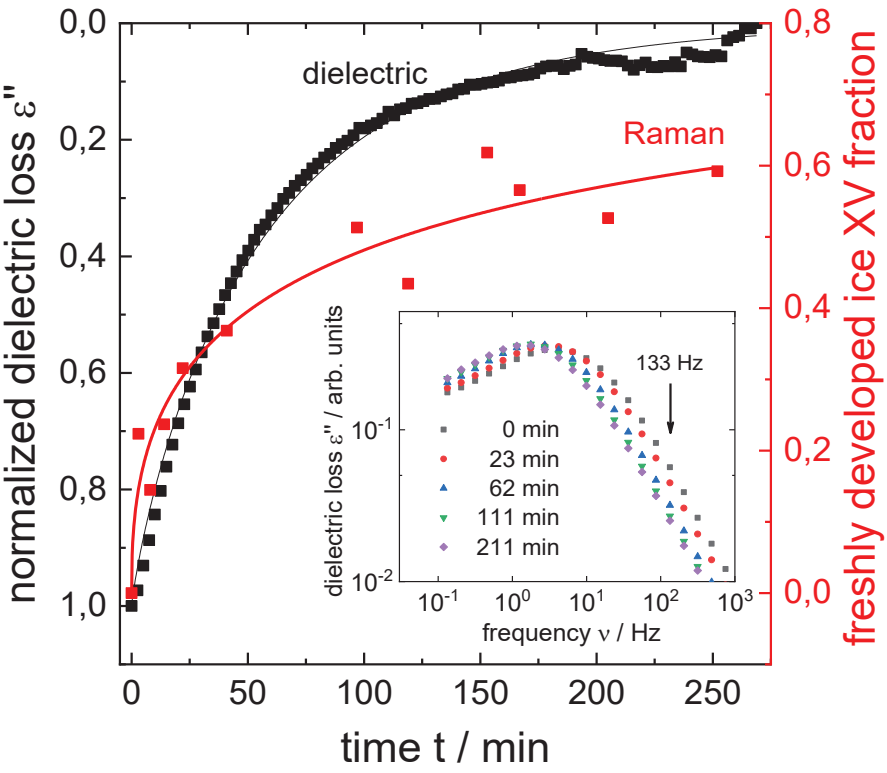

Figure S2: Avrami plot of a 95% H_2O sample based on the time dependent normalized dielectric loss at 133 Hz (left y-axis) and of the normalized Raman librational bands (right y-axis), both measured at 114 K. The inset shows the dielectric data as they were taken for different waiting times; the arrow marks a frequency of 133 Hz.

The rate constants derived from the JMAK fits to the dielectric and Raman spectra are relatively close to each other (*cf.* Table S1). The differences can be attributed to different heating rates. This suggests that both processes depicted in Fig. S2 are related to the ice VI‡ → XV transition. It is reassuring that the rate constants can consistently be determined using different methods. The blue diamond shown in the Arrhenius diagram, Fig. 4, represents the dielectric measurement depicted in Fig. S2.

An analogous isothermal waiting experiment was performed on a <0.04% H_2O sample. The results are shown in Fig. S3. As mentioned in Section 3.4, fully deuterated samples turn out to form hardly any ice XIX but they consist mainly of HCl doped H-disordered ice VI* [S3].

Figure S3 also includes Raman data referring to the ice VI‡ → XV transition as observed for a 5% H_2O sample. In Table S1 we compare the fit parameters obtained from the results of the two experiments. The dielectric Avrami exponent of 0.6 is well within the range of 0.2 to 1.1 that one infers from Table 2. The rate constant of 0.008 min^{-1} does not differ significantly from that derived from Raman spectra for ice the VI‡ → XV transition of the 5% H_2O sample at the same temperature. From this observation we conclude that a substantial difference between the kinetics of the ice VI* → XV transition and of the ice VI‡ → XV transition does not exist.

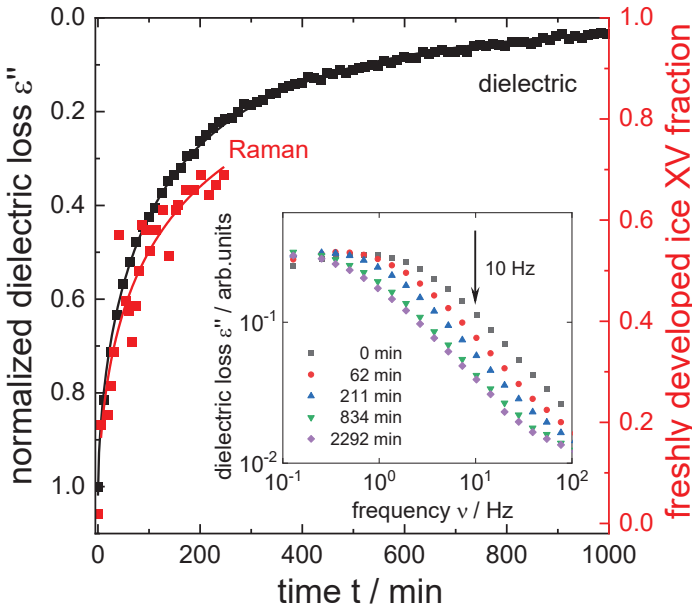

Figure S3: Avrami plot of a sample with <0.04% H_2O based on the time dependence of the normalized dielectric loss (left y-axis) recorded at 10 Hz and 114 K. The inset shows dielectric spectra taken for different waiting times. The right y-axis refers to results from Raman librational bands obtained for a somewhat less deuterated (5% H_2O) sample, again measured at 114 K.

The brownish diamond shown in the Arrhenius diagram, Fig. 4, represents the rate constant for the ice XV buildup that has been extracted from the dielectric data presented in Fig. S3.

Table S1: Kinetic parameters extracted for the ice XV buildup from isothermal waiting experiments carried out at 114 K using dielectric and Raman spectroscopy.

H_2O fraction	**method**	***k* / min^{-1}**	***n***
95%	dielectric	2×10^{-2}	0.9
95%	Raman	8×10^{-3}	0.4
<0.04%	dielectric	8×10^{-3}	0.6
5	Raman	6×10^{-3}	0.5

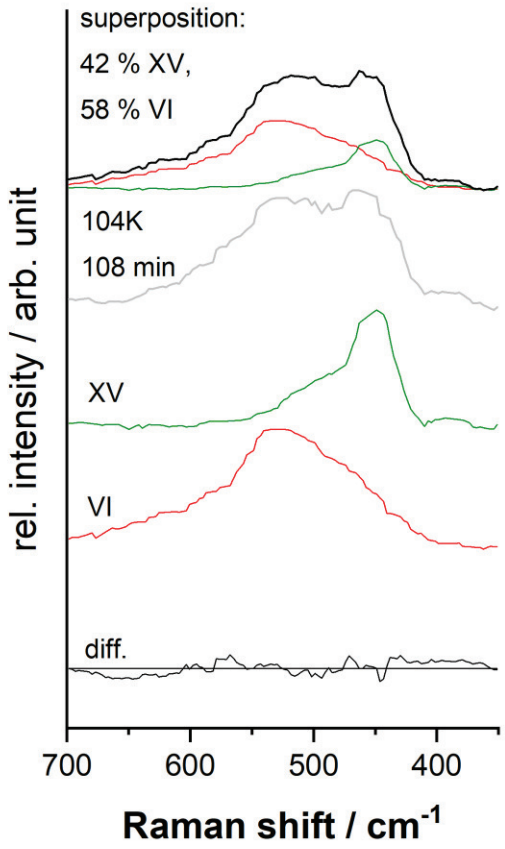

Figure S4: Superposition analysis of the librational range for the determination of the fractions of ice XV and ice VI. The spectrum recorded after 108 min at 104 K is depicted in the top line. The superposition is displayed in the line below. Reference spectra from pure ice VI (red) and ice XV (green) recorded at the same temperature are utilized. Each spectrum has been normalized to the most intense peak in the librational vibration range. The difference between the measured spectrum and calculated superposition is depicted in the bottom line.

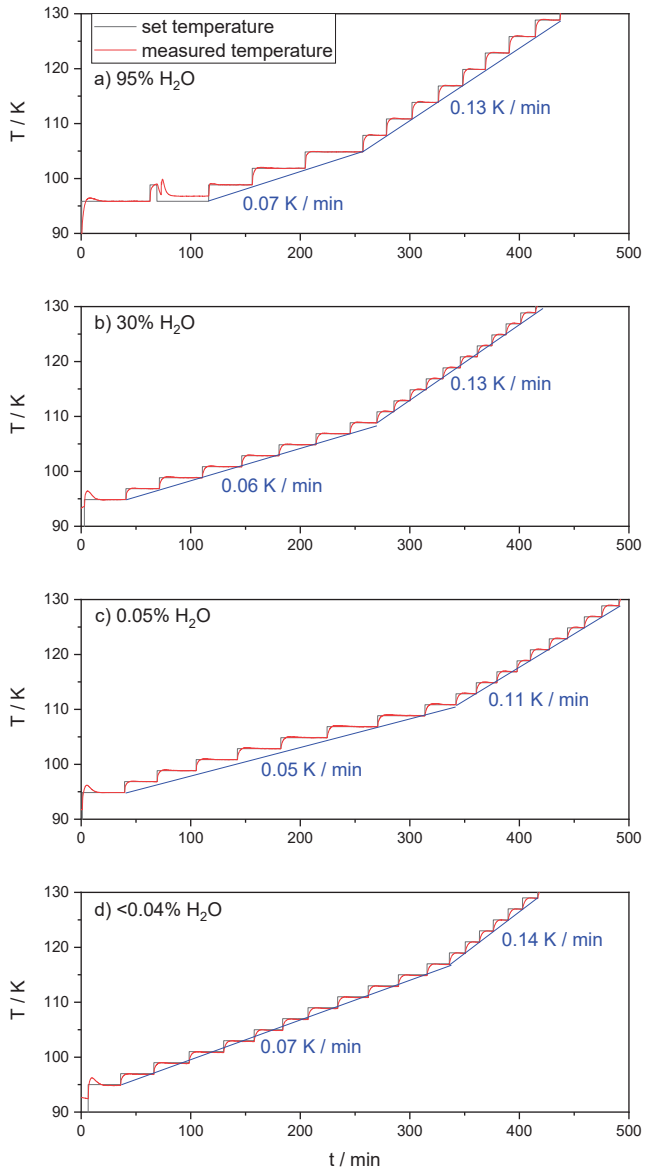

Figure S5: Heating protocol for dielectric measurements for the isotopic compositions 95% H_2O (a), 30% H_2O (b), 0.5% H_2O (c) and <0.04% H_2O (d) depicted in Figs. 5 and 6.

Supplementary References:

S1 S. Lemke, P.H. Handle, L.J. Plaga, J.N. Stern, M. Seidl, V. Fuentes-Landete, K. Amann-Winkel, K.W. Köster, C. Gainaru, T. Loerting, and R. Böhmer, *Relaxation dynamics and transformation kinetics of deeply supercooled water: Temperature, pressure, doping, and proton/deuteron isotope effects.* J Chem Phys, 2017. **147**(3). 034506 DOI: 10.1063/1.4993790.

S2 C. Gainaru, E. Vynokur, K.W. Köster, V. Fuentes-Landete, N. Spettel, J. Zollner, T. Loerting, and R. Böhmer, *Dynamic signatures of the transition from stacking disordered to hexagonal ice: Dielectric and nuclear magnetic resonance studies.* J. Chem Phys, 2018. **148**(13). 134502 DOI: 10.1063/1.5023178.

S3 T.M. Gasser, A.V. Thoeny, A.D. Fortes, and T. Loerting, *Structural characterization of ice XIX as the second polymorph related to ice VI.* Nat. Commun., 2021. **12**. 1128 DOI: 0.1038/s41467-021-21161-z.